



Published in final edited form as:

J Nanomed Nanotechnol. 2019 ; 10(6): . doi:10.35248/2157-7439.19.10.538.

Photophysical Studies of Ruthenium-Based Complexes and the Performance of Nanostructured TiO₂ Based Dye Sensitized Solar Cells

Meser M Ali¹, Wasif Pervez², William Ghann², Jamal Uddin^{2,*}

¹Department of Neurosurgery, Cellular and Molecular Imaging Laboratory, Henry Ford Hospital, Detroit, MI, USA

²Center for Nanotechnology, Department of Natural Sciences, Coppin State University, 2500 W. North Ave, Baltimore, MD, USA

Abstract

Dye-sensitized solar cells (DSSCs) have attracted enormous attention in the last couple of decades due to their relatively small size, low cost and minimal environmental impact. DSSCs convert solar energy to electrical energy with the aid of a sensitizing dye. In this work, two ruthenium-based dyes, tris(bipyridine)ruthenium(II) chloride (Rubpy) and ruthenium(II)2,2'-bis(benzimidazol-2-yl)-4,4'-bipyridine (RubbbpyH₂), were synthesized, characterized, and investigated for use as dye sensitizers in the fabrication of DSSCs. The photovoltaic performance of the ruthenium-based DSSCs was assessed. The solar-to-electric power efficiency of the RubbbpyH₂ DSSC was 0.2% and that of the Rubpy was 0.03%. The RubbbpyH₂ was also deprotonated and analyzed to study the effect of deprotonation on the efficiency of the solar cell. The deprotonated species, Rubbbpy, recorded an average efficiency of 0.12%. Thus, a change in pH did not enhance the efficiency of the solar cell. The cells were further characterized by impedance measurements. The photocurrent-photovoltage results were not consistent with the absorption spectra since Rubbbpy showed a more prominent band than RubbbpyH₂ but had a lower efficiency.

Keywords

TiO₂ nanoparticles; Solar cell; Ruthenium dye; DSSCs

INTRODUCTION

Among the different types of renewable energy that have been investigated recently, solar power is one of the most efficient and inexhaustible sources available [1]. Although solar panels have grown in use, concerns have also grown regarding the various risks and disadvantages associated with traditional silicon-based solar panels, such as cost and the

This is an open-access article distributed under the terms of the Creative Commons Attribution License, which permits unrestricted use, distribution, and reproduction in any medium, provided the original author and source are credited.

*Correspondence to: Jamal Uddin, Center for Nanotechnology, Department of Natural Sciences, Coppin State University, 2500 W. North Ave, Baltimore, MD, USA, Tel: +41213533380; Juddin@coppin.edu.

presence of toxic materials such as hexafluoroethane, lead, and polyvinyl fluoride. Dye-sensitized solar cells (DSSCs) have become attractive alternatives or complementary forms of solar cells owing to the fact that they are easily created, economical and fabricated with materials that are plentiful [2–4].

Work on DSSCs was first reported by O'Regan and Grätzel in 1991 [5]. Since then, there have been a plethora of publications dealing with the optimization of the various components of DSSCs with the goal of enhancing power conversion efficiency of the cells [6–12]. The DSSC is made up of three main parts: 1) a photoanode consisting of a sensitizing dye adsorbed on a semiconductor-coated fluorine doped tin oxide (FTO) glass; 2) an electrolyte made up of redox mediator; and 3) a counter electrode that facilitates redox reduction in the electrolyte.

In the presence of sunlight, the dye sensitizer absorbs photons leading to the ejection of an energized electron into the conduction band of the semiconductor. The injected electron is transported through the semiconductor to the conductive side of the FTO glass and subsequently through an external circuit to the counter electrode. At the counter electrode, the electron catalyzes the redox reaction in the electrolyte which in turn regenerates the oxidized dye. Thus, in DSSCs, charge separation occurs at the semiconductor-dye interfaces while the transport of charge is performed by the semiconductor and the electrolyte. This arrangement allows for optimization of the spectral properties to be carried out by modification of the dye alone. Similarly, the charge transport properties of the device could be enhanced by the optimization of the semiconductor and the electrolyte composition [13–15]. The many channels through which DSSCs can be optimized has given rise to a large number of papers reporting on studies carried out to improve the efficiency of the DSSC.

One particular area that has occupied the interest of most researchers is the dye sensitizers used in the solar cell. Both synthetic and natural dyes have been used with notable success. Natural dyes obtained from different parts of plants have been used in the fabrication of solar cells [16–21]. Although natural dyes are more environmentally friendly, low cost, and abundant in supply, their efficiencies are not as high as that of most synthetic dyes.

Dyes that have been synthesized and applied in DSSCs include ruthenium complexes, [22,23] Porphyrin dyes, [24] and Cyanine dyes [25]. Among these groups, DSSCs using ruthenium complex dyes have consistently produced the best results due to their relatively long life in metal-to-ligand charge transfer (MLCT) properties. Most studies have reported using ruthenium trisbipyridin complexes as molecular devices for energy conversion. The modification or tuning of redox and photochemical properties have been reported by replacing bipyridin ligand with other nitrogen-containing heterocycles [26]. In addition, pH-dependent redox and photochemical properties have been reported in a ruthenium benzimidazole-based complex where imidazole moiety functions as a pH sensor [26]. In the present study, several ruthenium complexes containing bridging ligand 2,2'-bis(benzimidazol-2-yl)-4,4'-bipyridine (bbbpyH_2) and 2,2'-bipyridine (Scheme 1) have been used as sensitizers for the fabrication of DSSCs.

The optical and structural properties of the dyes and the fabricated DSSCs were investigated. Also, the efficiencies of the fabricated solar cells were investigated via current and voltage measurement as well as by impedance spectroscopy, which examines the interface between the dye and TiO₂.

EXPERIMENTAL SECTION

Materials

Titanium dioxide powder (Degussa P-25) was purchased from the Institute of Chemical Education, University of Wisconsin-Madison, Department of Chemistry, Madison, WI, USA. Fluorine tin oxide (FTO) coated glass slides were purchased from Hartford Glass Company, Hartford City, Indiana, USA. Sodium hydroxide (NaOH), ethanol (C₂H₅OH) and acetic acid (CH₃CO₂H) were purchased from Sigma-Aldrich (St. Louis, MS, USA) and were used without further purification.

Characterization techniques

Absorption spectroscopy was carried out with UV-3600 Plus from Shimadzu, MD, USA. Emission spectroscopy was measured with RF-5301PC from Shimadzu, MD, USA. TiO₂ paste was printed on FTO glass using WS-650 Series Spin Processor from Laurell Technologies Corporation, PA, USA. Carbon paint used in making cathode slides was purchased from Ted Pella, Inc., USA. The cell performance was measured using a 150 W fully reflective solar simulator with a standard illumination of air-mass 1.5 global (AM 1.5 G) having an irradiance of 100mW/cm² (Sciencetech, Inc.) from London, Ontario, Canada. Reference 600 Potentiostat/Galvanostat/ZRA was purchased from GAMRY Instruments (Warminster, PA).

Fabrication of DSSCs

The electrodes were prepared according to a previously published procedure with some modifications [27–30]. The working electrode was prepared by depositing a thin film of TiO₂ on the conductive side of a fluorine doped tin oxide (FTO) glass slide using a spin coater and the film annealed at 380 °C for 2 hours. The substrate was then immersed in dye for sensitization. The counter electrode (cathode) was prepared by printing colloidal graphite on FTO coated glass slide. The dye-sensitized slide and the carbon electrodes were assembled to form a solar cell by sandwiching a redox (I⁻/I₃⁻) electrolyte solution.

Synthesis of the bridging ligand 2,2'-bis(benzimidazol-2-yl)-4,4'-bipyridine (bbbpyH₂)

The synthesis of bridging ligand 2,2'-bis(benzimidazol-2-yl)-4,4'-bipyridine (bbbpyH₂) and its ruthenium complex was reported in details by Haga et al. [26].

RESULT AND DISCUSSION

UV Vis measurements

The UV-Vis measurement of the Rubpy, RubbbbpyH₂ and Rubbbbpy (deprotonated form) were carried out to study the effect of absorption on the efficiency of the corresponding solar cell. The UV-vis spectrum of the Rubpy and RubbbbpyH₂ show single absorption peaks at 450 and

463 nm, respectively, as displayed in Figure 1. The UV-Vis of the Rubbbpy, however, is broad and exhibited dual peaks at 450 and 472 nm.

Steady state fluorescence studies

The steady state fluorescence spectra of the three dyes were taken as part of the photophysical studies on the dyes and are displayed in Figure 2. The measurements were carried out in ethanol with an exciting light of 600 nm. The emission maximum of Rubpy at 594 nm and that of the Rubbbpy is 641 nm but is red-shifted and broadened in the case of the deprotonated species.

Fluorescence Lifetime measurement

Fluorescence emission decay curves of the Rubpy, RubbbpyH₂ and Rubbbpy were measured and the results are displayed in Figure 3 and Table 1. The measurements were conducted in ethanol. The results were fitted to the second exponential decay with a faster component of 22 ps, 13.4 ps, and 7.7 ps and a slower component of 347 ns, 332 ns, and 352 ns for the Rubpy, RubbbpyH₂ and Rubbbpy, respectively. The values obtained are well within the lifetime values of 200-800 ns reported by Haga et al. [26] for mono- and dinuclear Ru complexes at room temperature. Dinuclear Ru complexes were specifically found to have a higher lifetime, however, water decreased the lifetime drastically. This decrease is attributed to the hydrogen-bonding interaction of the imino NH moiety of bbbpyH₂ which acts as H⁺ donor and the water as H⁺ acceptor. Thus using ethanol as the solvent likely resulted in the lower lifetime due to the change in the excited-state properties.

Fourier-transform infrared spectroscopy studies of dye-sensitized photoanode

Fourier-transform infrared spectroscopy (FTIR) studies were carried out to investigate the interaction of the TiO₂ with different dyes that were utilized. The dyes usually need specific functional groups to effectively adsorb on the TiO₂ film. In the presence of such functional groups, the dye adsorbs firmly to the titanium dioxide which results in the easy transport of charge and consequently a higher efficiency of the solar cell. The FTIR spectra of blank TiO₂, Rubpy, RubbbpyH₂ and Rubbbpy dye-sensitized titanium dioxide film are displayed in Figure 4. The peak at 3440 cm⁻¹ is due to the presence of the hydroxyl group in the Rubbbpy.

Raman studies of dye-sensitized photoanode

The Raman spectra of the dyes with titanium dioxide were measured to study the interaction of the dye with titanium dioxide. A comparison between Raman spectra of Rubpy dye, RubbbpyH₂ and Rubbbpy with titanium dioxide was evaluated. Figure 5 shows spectra of the dyes adsorbed on the TiO₂ surface, which is consistent with the Raman spectra of a typical ruthenium complex dye adsorbed to a titanium dioxide surface. The three bands at 395 cm⁻¹, 513 cm⁻¹, and 635 cm⁻¹ are characteristic of the titanium dioxide. Two Raman spectra showing the characteristic bands at 1610 cm⁻¹ and 1544 cm⁻¹ are consistent with the ruthenium-based dyes.

Current-voltage characteristics of Rubpy, Rubbbpy, and RubbbpyH₂ DSSCs

The current-voltage characteristics of the samples under simulated solar irradiation of AM 1.5 G were carried out to study the differences in the efficiency of solar cells. The results of the photocurrent-voltage measurements are displayed in Figure 6 and Table 2. The solar-to-electric power efficiency of the Rubpy DSSC was 0.029% whereas that of Rubbbpy, and RubbbpyH₂ DSSCs was 0.118% and 0.201%, respectively. With deprotonation using sodium methoxide, the expectation was an improved interaction of the dye with titanium dioxide resulting in a higher efficiency. However, the efficiency of the RubbbpyH₂ was found to be higher than that of the DSSCs of the deprotonated species. Thus, whereas the binding might have improved, it did not translate into a higher yield of the electric power.

Electrochemical impedance spectroscopy

Electrical impedance spectroscopy (EIS) is an important electrochemical technique normally used for investigation of charge carrier dynamics in DSSCs. EIS was employed in this work to characterize the three different DSSC samples. The results of the EIS measurement are presented in a Nyquist plot in Figure 7 and in a Bode plot in Figure 8. The measurements were undertaken in the frequency range of 0.01 Hz to 100 KHz. The two semicircles displayed in the Nyquist plot indicate the electron transfer processes between the dye-sensitized photoanode and the electrolyte interface.

CONCLUSION

The photovoltaic performance of the RubpyCl₂ DSSC was compared to that of RubbbpyH₂ and its deprotonated form to study the effect of the imidazole group and pH on the efficiency of solar cells. The dyes were first characterized with UV-Vis, Emission Spectroscopy and Lifetime measurements. The solar cell efficiency of the Rubpy was 0.029% and that of the RubbbpyH₂ was 0.20%. The efficiency of the Rubbbpy was 0.118%. Although the effect of the pH was evident in the photophysical studies, there was no significant change in the photovoltaic properties of the resulting DSSCs.

ACKNOWLEDGEMENT

This study was funded by the University of Maryland System (Wilson E. Elkins Professorship), Constellation, an Exelon Company (E2-Energy to Educate grant program) and the United States Department of Education (USDE-SAFRA Title III Grant). The authors extend special thanks to the office of Institutional Advancement, Coppin State University, for administrative support. The content is exclusively the responsibility of the authors and does not necessarily represent the official views of the funding agencies. The authors also acknowledge research support from the National Institutes of Health (NIH) grant RO1CA206190 to MMA.

REFERENCES

1. Kannan N, Vakeesan D. Solar energy for future world: - A review. *Renewable and Sustainable Energy Reviews*. 2016;62:1092–1105.
2. Singh GK. Solar power generation by PV (photovoltaic) technology: A review. *Energy*. 2013;53:1–13.
3. Shalini S, Balasundara prabhu R, Prasanna S, Mallick TK, Senthilarasu S. Review on natural dye sensitized solar cells: Operation, materials and methods. *Renew Sust Energ*. 2015;51:1306–1325.
4. Sugathan V, John E, Sudhakar K. Recent improvements in dye sensitized solar cells: A review. *Renew Sust Energ Rev*. 2015;52:54–64.

5. O'Regan B, Gratzel M. A low-cost, high-efficiency solar cell based on dye-sensitized colloidal TiO₂ films. *Nature*. 1991;353:737–740.
6. Bach U, Lupo D, Comte P, Moser JE, Weissortel F, Salbeck J, et al. Solid-state dye-sensitized mesoporous TiO₂ solar cells with high photon-to-electron conversion efficiencies. *Nature*. 1998;395:583–585.
7. Boschloo G, Hagfeldt A. Characteristics of the iodide/triiodide redox mediator in dye-sensitized solar cells. *Acc Chem Res* 2009;42:1819–1826. [PubMed: 19845388]
8. Cao YM, Liu YH, Zakeeruddin SM, Hagfeldt A, Gratzel M. Direct contact of selective charge extraction layers enables high-efficiency molecular photovoltaics. *Joule* 2018;2:1108–1117.
9. Cappel UB, Gibson EA, Hagfeldt A, Boschloo G (2009) Dye regeneration by spiro-MeOTAD in solid state dye-sensitized solar cells studied by photoinduced absorption spectroscopy and spectroelectrochemistry. *J Phys Chem C* 113:6275–6281.
10. Ellis H, Jiang R, Ye S, Hagfeldt A, Boschloo G. Development of high efficiency 100% aqueous cobalt electrolyte dye-sensitized solar cells. *Phys Chem Chem Phys*. 2016;18:8419–8427. [PubMed: 26931779]
11. Feldt SM, Gibson EA, Gabrielsson E, Sun L, Boschloo G, Hagfeldt A. Design of organic dyes and cobalt polypyridine redox mediators for high-efficiency dye-sensitized solar cells. *J Am Chem Soc* 2010;132:16714–16724. [PubMed: 21047080]
12. Yoo K Completely Transparent Conducting Oxide-Free and Flexible Dye-Sensitized Solar Cells Fabricated on Plastic Substrates. *ACS Nano*. 2015;9:3760–3771. [PubMed: 25769343]
13. Qu Q, Geng H, Peng R, Cui Q, Gu X, Li F, et al. Chemically Binding Carboxylic Acids onto TiO₂ Nanoparticles with Adjustable Coverage by Solvothermal Strategy. *Langmuir*. 2010;26(12):9539–9546. [PubMed: 20345108]
14. Nazeeruddin MK, Baranoff E, Grätzel M. Dye-sensitized solar cells: A brief overview. *Solar Energy*. 2011;85(6):1172–1178.
15. Hug H, Bader M, Mair P, Glatzel T. Biophotovoltaics: Natural pigments in dye-sensitized solar cells *Appl. Energy*. 2014;115:216–225.
16. Ludin NA. Review on the development of natural dye photosensitizer for dye-sensitized solar cells. *Renew Sust Energ*, 2014;31:386–396.
17. Chang H, Kao MJ, Chen TL, Chen CH, Cho KC, Lai XR, et al. Characterization of natural dye extracted from wormwood and purple cabbage for dye-sensitized solar cells. *International Journal of Photoenergy*. 2013;159502.
18. Ganta D, Jara J, Villanueva R. Dye-sensitized solar cells using aloe vera and cladode of cactus extracts as natural sensitizers. *Chem Phy Lett* 2017;679:97–101.
19. Kushwaha R, Srivastava P, Bahadur L. Natural pigments from plants used as sensitizers for TiO₂ based dye-sensitized solar cells. *J Energy*. 2013; ID 654953.
20. Richhariya G, Kumar A, Tekasakul P, Gupta B. Natural dyes for dye sensitized solar cell: A review. *Renew Sustain Ene Rev*. 2017;69:705–718.
21. Rossi M, Matteocci F, Di Carlo A, Forni C. Chlorophylls and xanthophylls of crop plants as dyes for dye-sensitized solar cells (DSSC). *J Plant Sci Phytopat*. 2017;1:87–94.
22. Ammar AM, Mohamed HSH, Yousef MMK, Abdel-Hafez GM, Hassanien AS, Khalil ASG. Dye-Sensitized Solar Cells (DSSCs) Based on Extracted Natural Dyes. *Journal of Nanomaterials*. 2019.
23. Oh J, Ghann W, Kang H, Nesbitt F, Providence S, Uddin J. Comparison of the performance of dye sensitized solar cells fabricated with ruthenium based dye sensitizers: Di-tetrabutylammonium cisbis(isothiocyanato)bis(2,2'-bipyridyl-4,4'-dicarboxylato)ruthenium(II) (N719) and tris(bipyridine)ruthenium(II) chloride (Ru-BPY), *Inorganica Chimica Acta*, 2018;482:935–943.
24. Ghann W, Chavez-Gil T, Goede CI, Kang H, Khan S, Sobhi H, et al. Photophysical, Electrochemical and Photovoltaic Properties of Porphyrin-Based Dye Sensitized Solar Cell. *Advances in Materials Physics and Chemistry*. 2017;7:148–172.
25. Ghann W, Kang H, Emerson E, Oh J, Chavez-Gil T, Nesbitt F, et al. Photophysical properties of near-IR cyanine dyes and their application as photosensitizers in dye sensitized solar cells. *Inorganica Chimica Acta*, 2017;467:123–131.
26. Haga M, Ali MM, Koseki S, Fujimoto K, Yoshimura A, Nozaki K, et al. Proton-Induced Tuning of Electrochemical and Photophysical Properties in Mononuclear and Dinuclear Ruthenium

Complexes Containing 2,2'-Bis(benzimidazol-2-yl)-4,4'-bipyridine: Synthesis, Molecular Structure, and Mixed-Valence State and Excited-State Properties. *Inorg Chem.* 1996;35(11):3335–3347. [PubMed: 11666536]

27. Ghann W, Kang H, Sheikh T, Yadav S, Chavez-Gil T, Nesbitt F, et al. Fabrication, Optimization and Characterization of Natural Dye Sensitized Solar Cell. *Sci Rep.* 2017;7(1).
28. Ghann W, Kang H, Uddin J, Gonawala SJ, Mahatabuddin S. Dendrimer-based Nanoparticle for Dye Sensitized Solar Cells with Improved Efficiency. *J Nanomed Nanotechnol.* 2018.
29. Ghann WE, Kang H, Uddin J, Chowdhury FA, Khondaker SI, Moniruzzaman M, et al. Synthesis and Characterization of Reduced Graphene Oxide and Their Application in Dye-Sensitized Solar Cells. *Chem Eng.* 2019;3:7.
30. Ghann W, Sharma V, Kang H, Karim F, Richards B, Mobin SM, et al. The synthesis and characterization of carbon dots and their application in dye sensitized solar cell, *International Journal of Hydrogen Energy*, 2019;44:14580–14587.

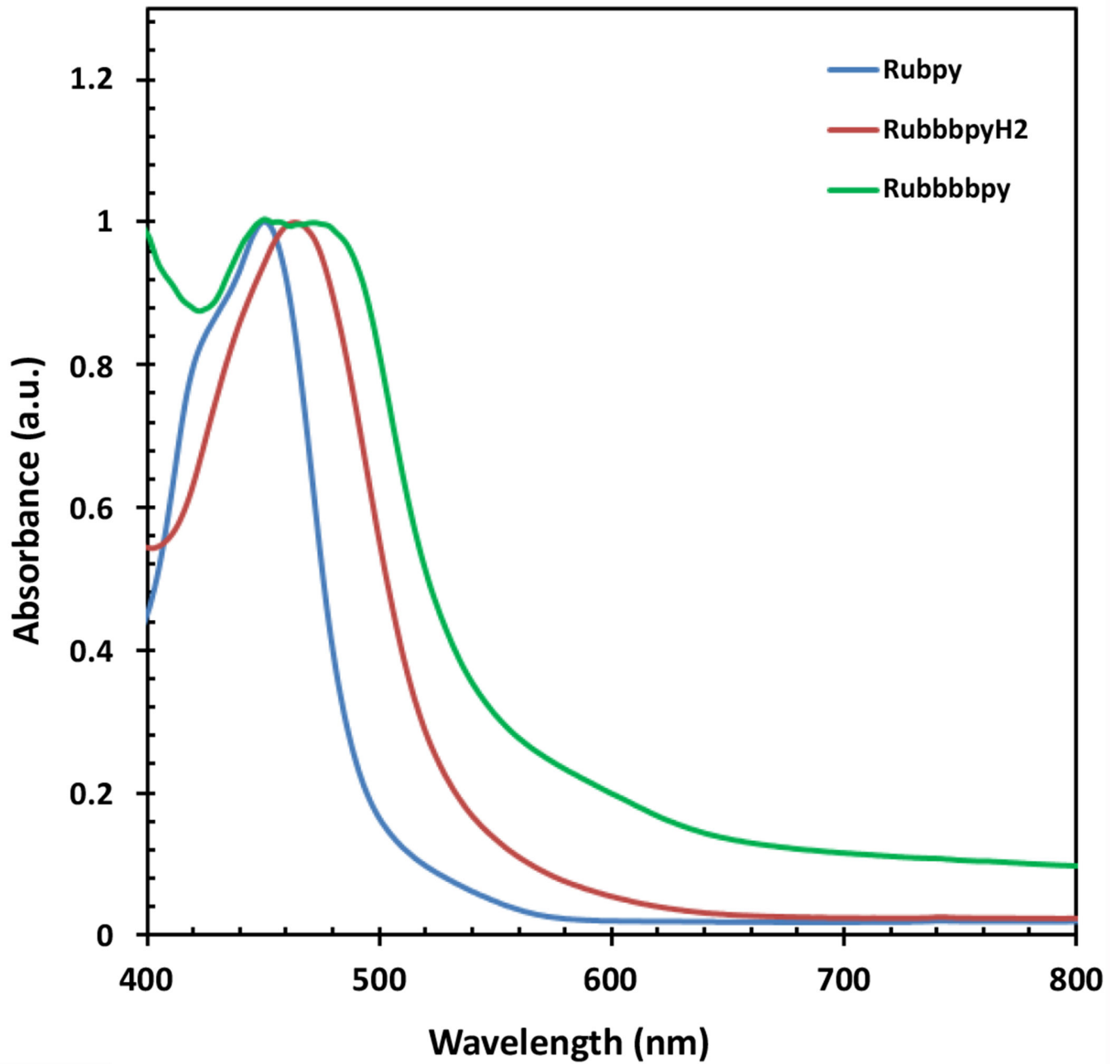


Figure 1:
Absorption spectra of Rubpy, RubbbpyH₂ and Rubbbpy in ethanol.

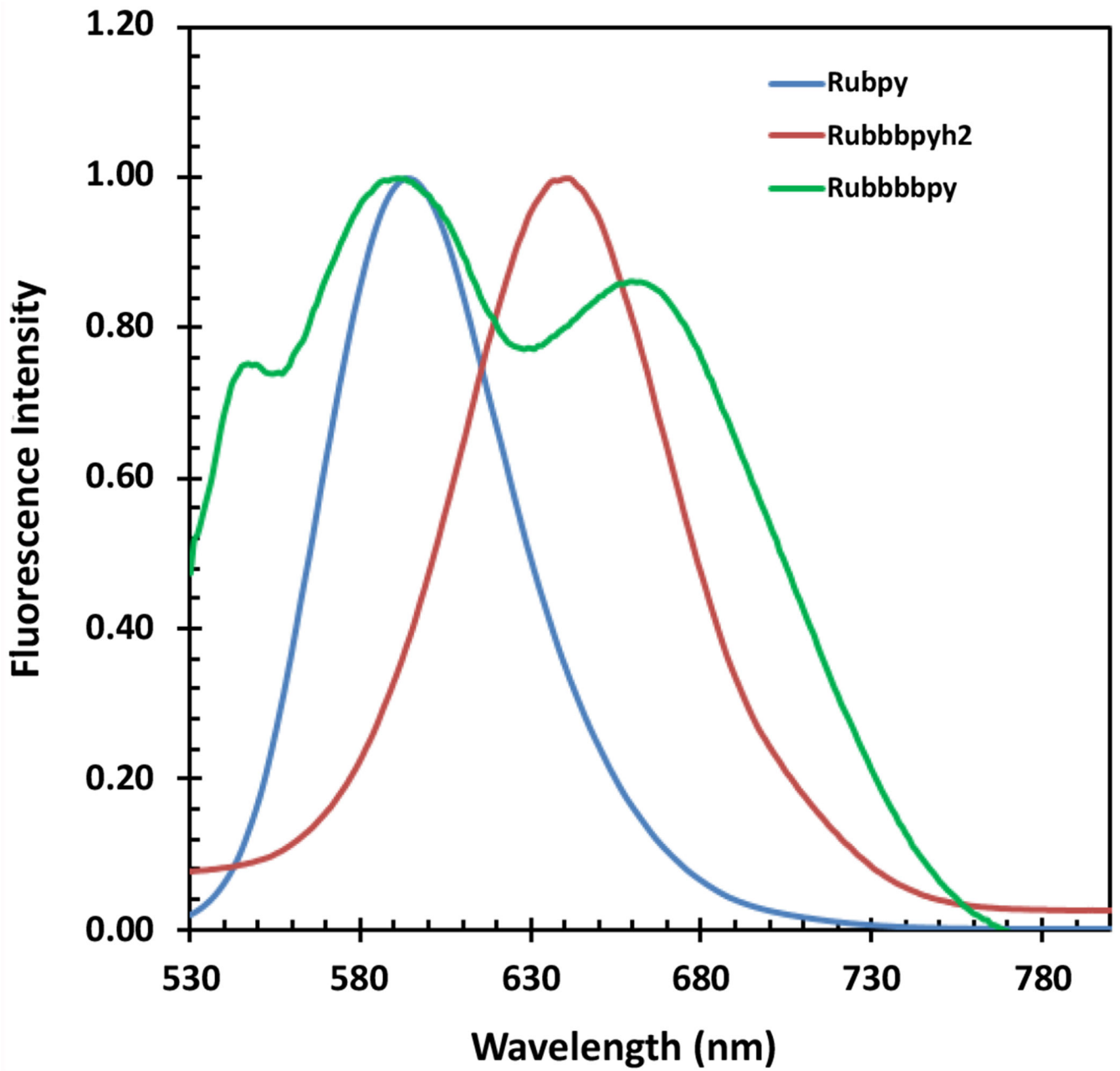


Figure 2:
Emission spectra of Rubpy, RubbbpyH₂ and Rubbbpy.

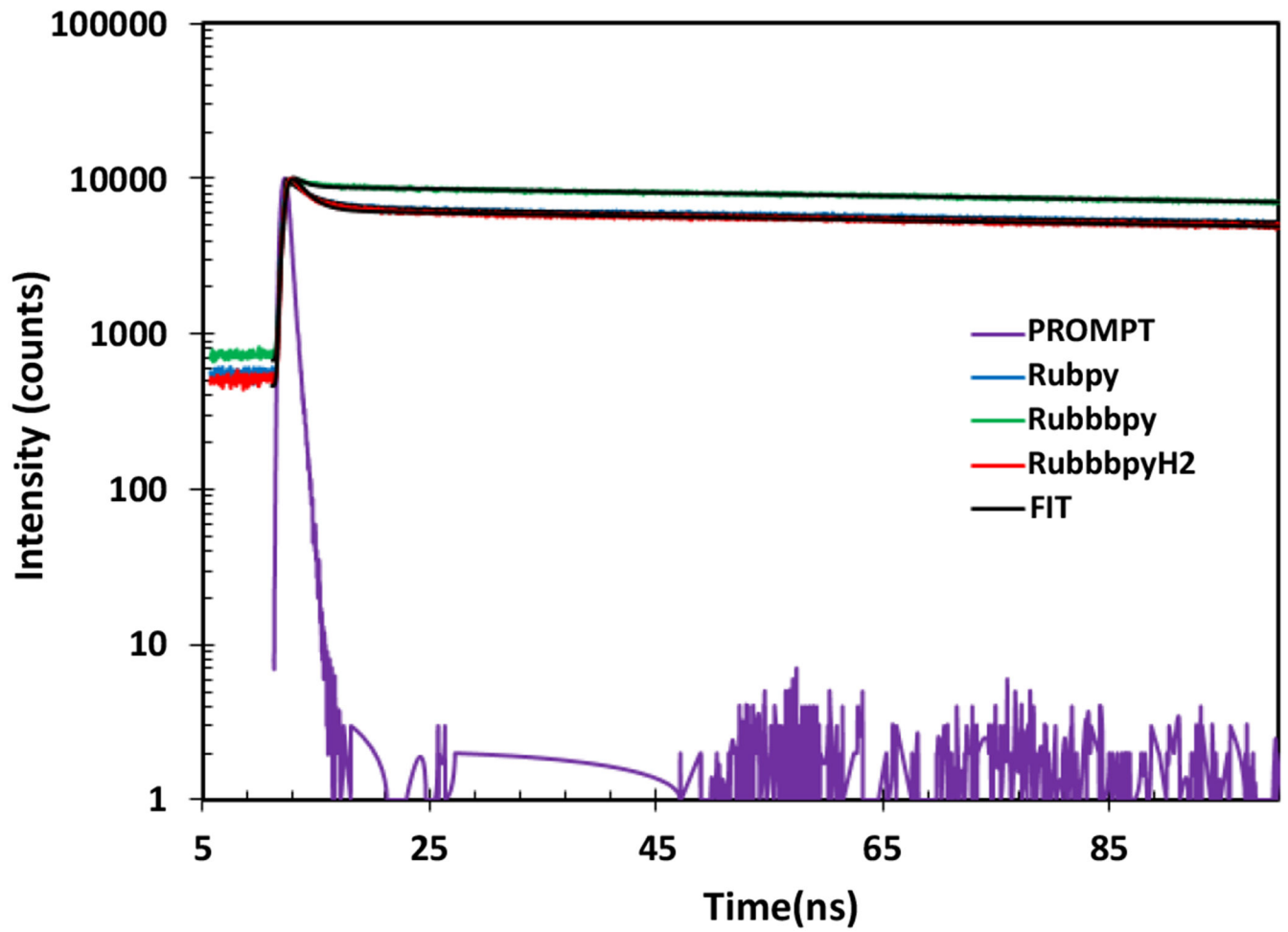


Figure 3:
Lifetime measurements of Rubpy, RubbppyH₂ and Rubbppy.

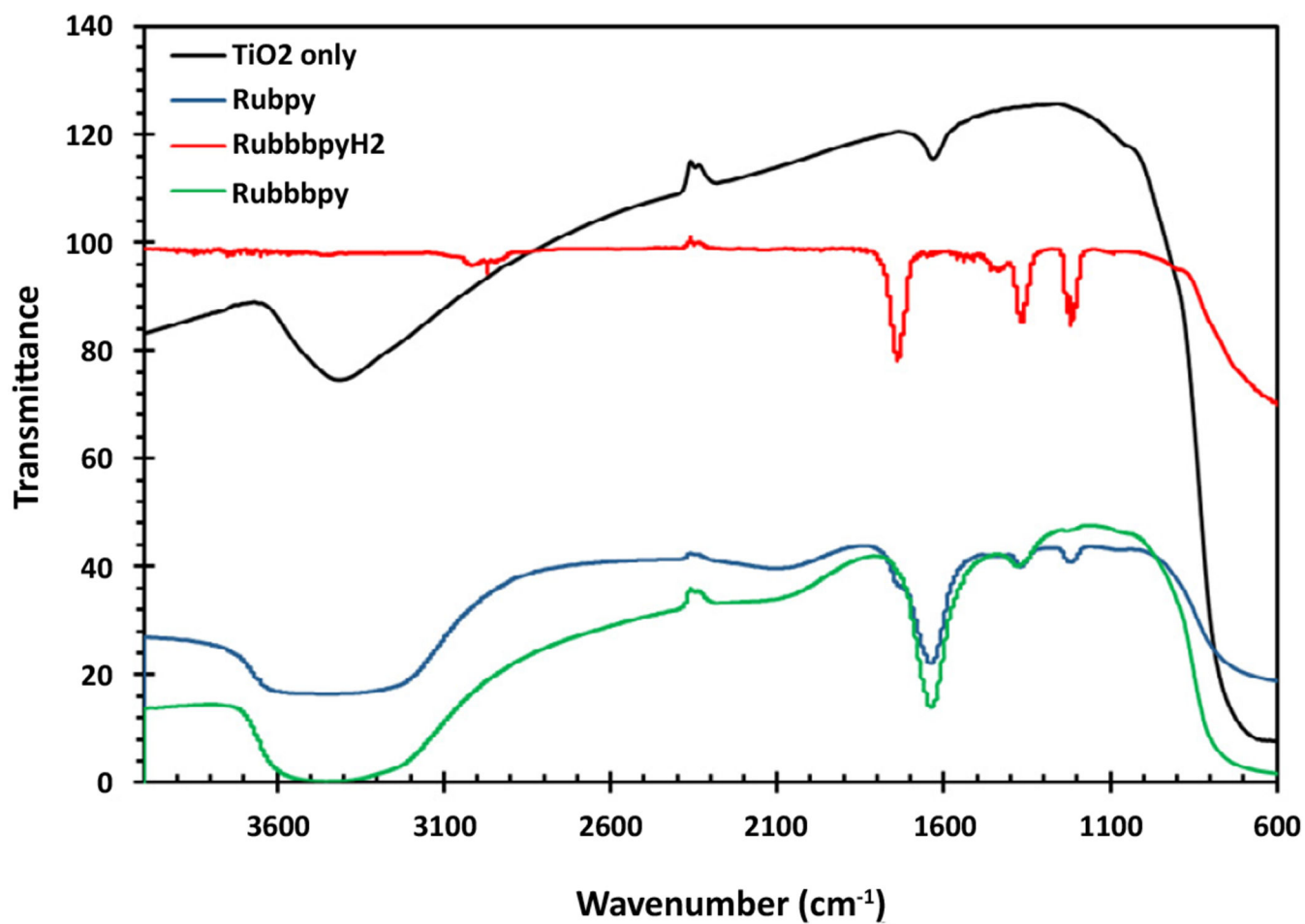


Figure 4:
FTIR Spectra of the Rubpy, RubbpyH₂ and Rubbpy sensitized TiO₂ compared to that of blank TiO₂.

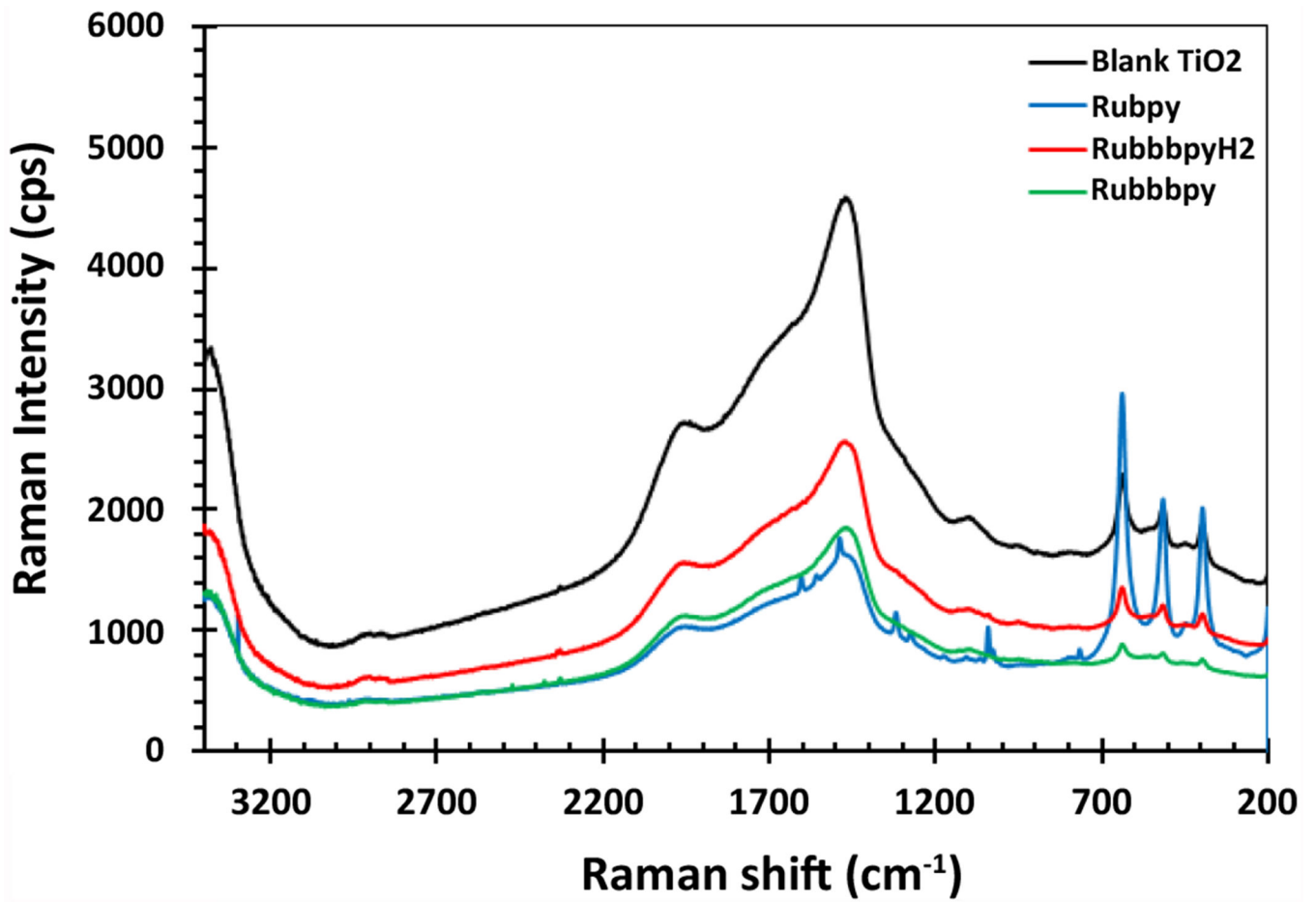


Figure 5:
Raman Spectra of the Rubpy, RubbbpyH₂ and Rubbbpy sensitized TiO₂ compared to that of blank TiO₂.

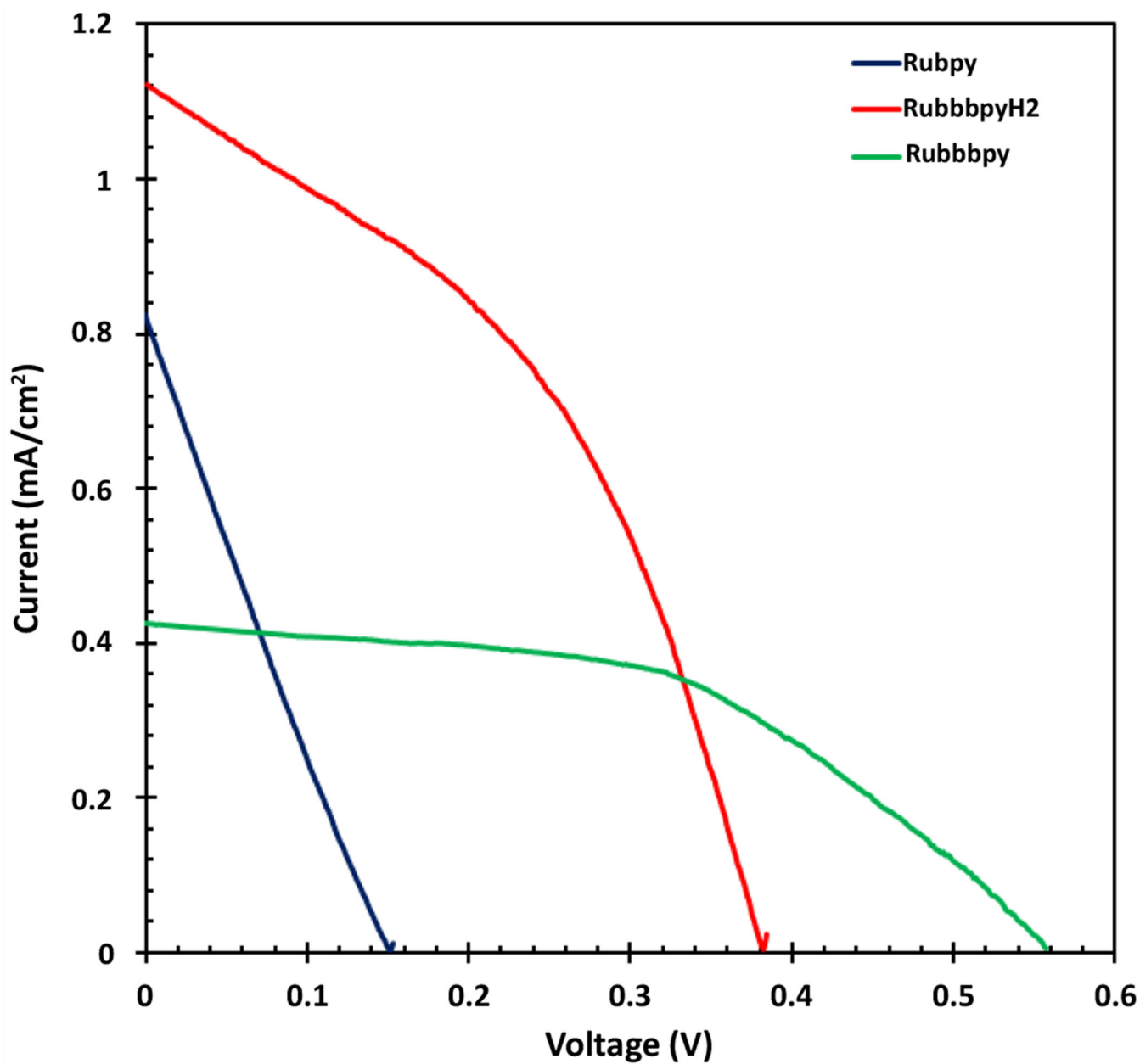


Figure 6: Photocurrent-voltage characteristics of Rubpy, Rubbbpy, and RubbbpyH₂ dye- sensitized solar cells measured under illumination of 100 mW/cm² (1.5 AM).

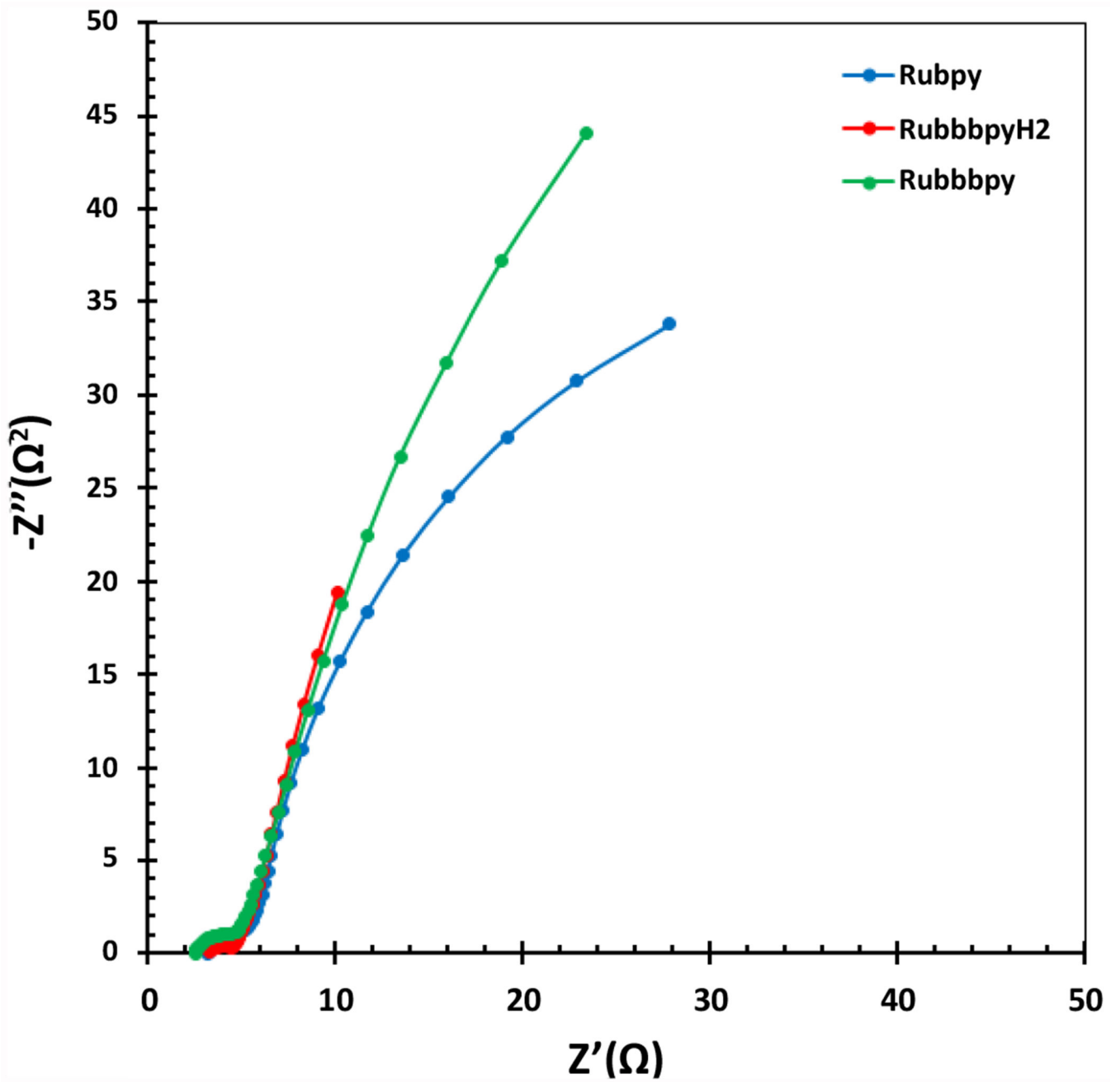


Figure 7: Nyquist plots for the fabricated Rubpy, Rubbbpy, and RubbbpyH₂ dye sensitized solar cells showing differences in the resistance to charge transfer.

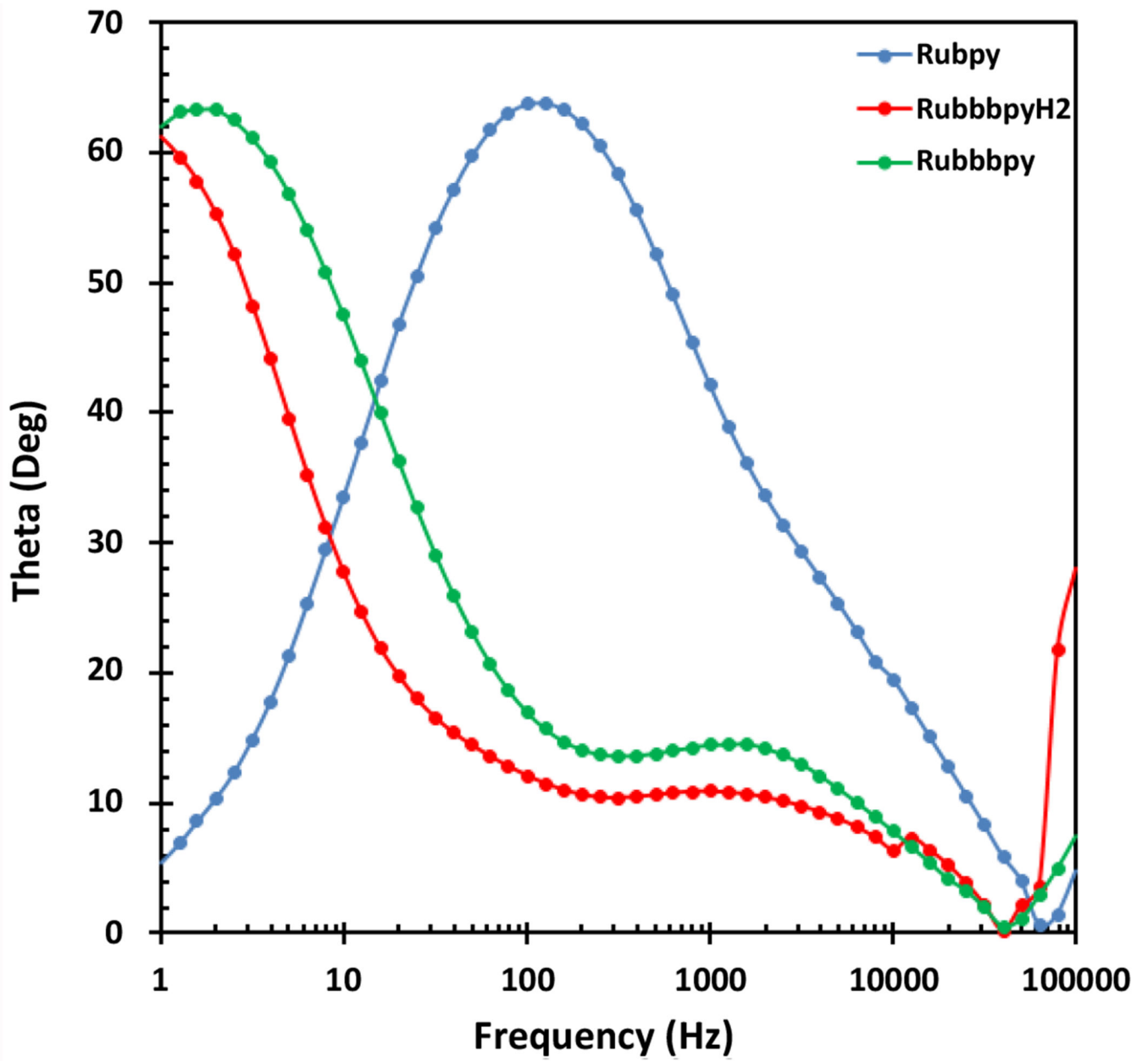
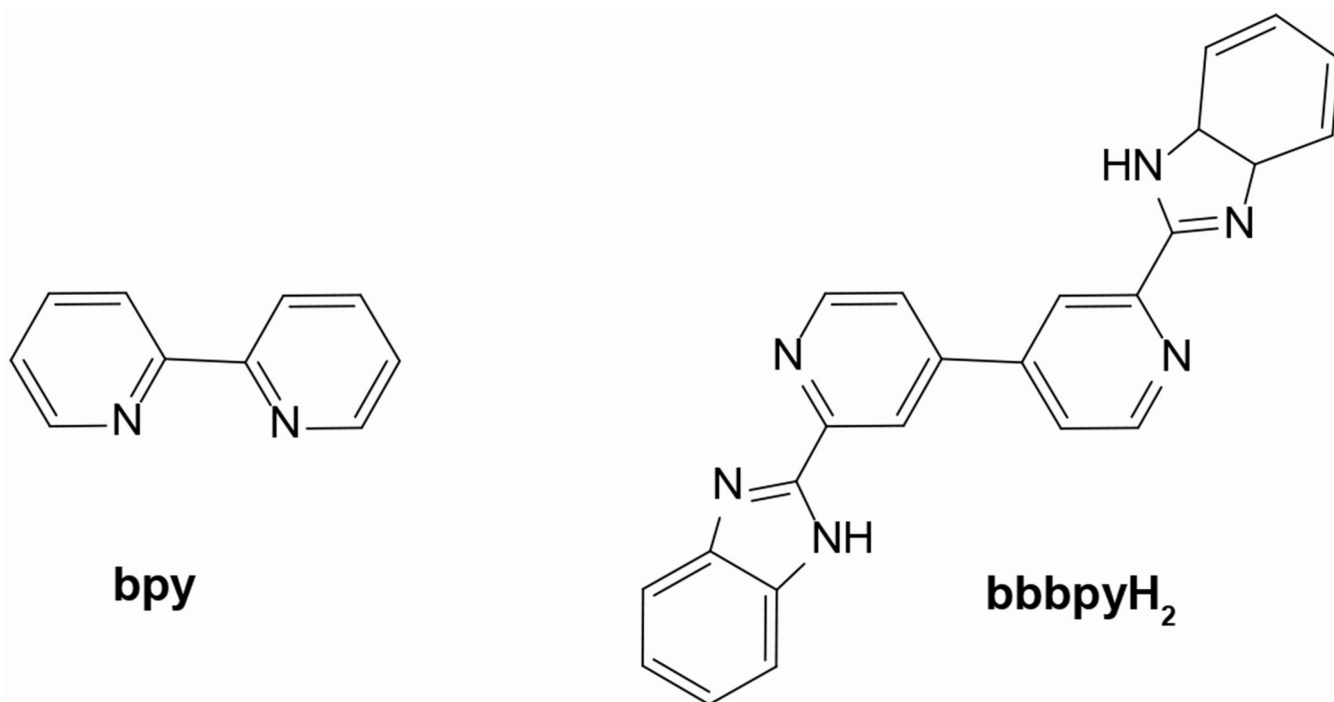


Figure 8: Bode plots for the fabricated Rubpy, Rubbbpy, and RubbbpyH₂ dye sensitized solar cells.



Scheme 1:
Schematic view of 2,2'-bipyridine (bpy) and bridging ligand 2,2'-bis(benzimidazol-2-yl)-4,4'-bipyridine (bbbpyH₂).

Table 1:Fluorescence lifetime measurement of Rubpy, RubbppyH₂ and Rubbppy.

Sample	Lifetime	Standard Deviation (σ)	Lifetime	Standard Deviation (σ)
	(τ_1) (ps)		(τ_1) (ns)	
Rubpy	22	2.47E-12	347	1.84E-09
RubbppyH ₂	13.4	1.93E-11	332	1.44-9
Rubbppy	7.7	2.1E-12s	352	2.70E-11

Author Manuscript

Author Manuscript

Author Manuscript

Author Manuscript

Table 2:

Current voltage characteristics of Rubpy, RubbbpyH₂ and Rubbbpy dye-sensitized solar cells.

	V _{oc}	I _{SC} (mA/cm ²)	V _{mp}	I _{mp} (mA/cm ²)	Fill Factor (%)	Efficiency (%)
	(V)		(V)			
Rubpy	0.15	0.83	0.07	0.41	0.23	0.03
RubbbpyH ₂	0.38	1.04	0.25	0.8	0.5	0.2
Rubbbpy	0.56	0.43	0.35	0.34	0.5	0.12

Author Manuscript

Author Manuscript

Author Manuscript

Author Manuscript